Iterative tomography: addendum

Marta Jo Woodward

INTRODUCTION

This paper is an addendum to "Iterative tomography: error projection along ellipses and lines" (Woodward, 1986). It includes that material presented at Fallen Leaf Lake in May 1986 on crosshole tomography and finite-aperture-induced artifacts which did not appear in SEP-48. The paper is divided into three parts: first, a Fourier domain examination of backprojection artifacts for the three different inversion schemes described in the previous paper; second, a comparison of artifacts resulting from application of two of the schemes (backprojection along narrow and wide raypaths) to a new, flat-layered model; third, a figure correction.

ARTIFACTS IN THE FOURIER DOMAIN

Figures 1a and 2a are repeated from Figures 1 and 2 in SEP-48, showing, respectively, a crosshole experiment with a central high velocity anomaly and the fifth iteration in an ART inversion of the crosshole traveltimes. The latter corresponds to the first inversion scheme of the previous paper, where slowness errors were backprojected along narrow raypaths. The finite aperture of the experiment and the narrow backprojections of the inversion limited the linkage between the cells, producing x-shaped artifacts and a horizontal smearing of the result in the space domain. The relation between these artifacts and the finite aperture of the experiment is made more clear by comparing the model and the ART solution in the spatial frequency domain. Figures 1b and 2b show the amplitude spectra for the model and the narrow-raypath ART solution as contour plots, with the k_x and k_z axis origins in the centers. Besides losing high frequency content in the x-direction—which was to be expected since slowness perturbations were backprojected more or less horizontally—the ART method also produced a notch, or pie-slice-filtering effect along the $k_z = 0$ axis. The presence of this notch is explained by the projection-slice theorem, which states that the one-dimensional Fourier transform of a projection at an angle θ through an object is a slice at the same angle through the two-dimensional Fourier transform of the object (Bracewell, 1956). (See Figure 3.) Because the crosshole experiment yielded only vertical or

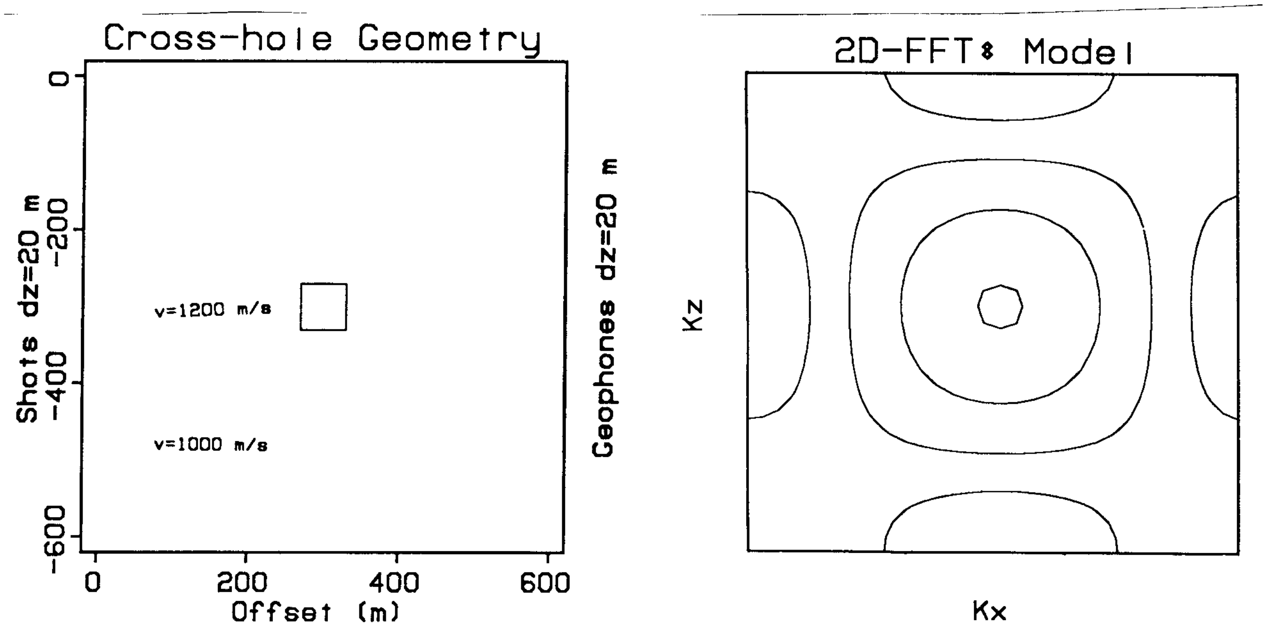

FIG. 1. (a): A crosshole tomography experiment with a central velocity anomaly. (b): The amplitude spectrum of (a).

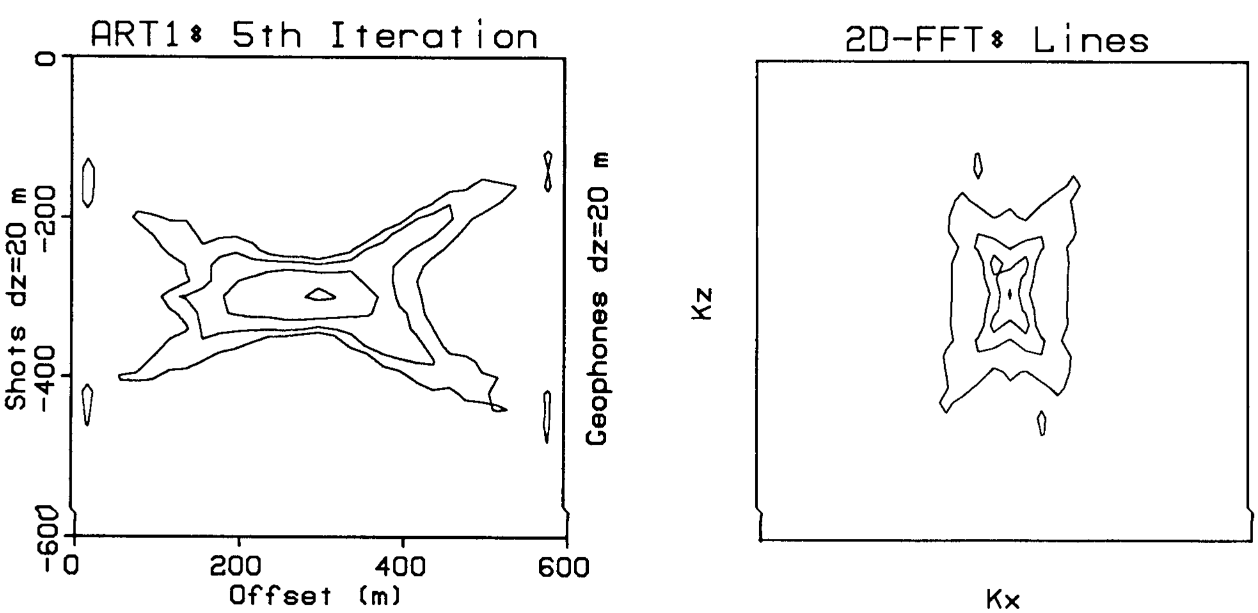

FIG. 2. (a): The fifth iteration in an ART solution to the tomography problem posed in Figure 1a. (b): The amplitude spectrum of (a).

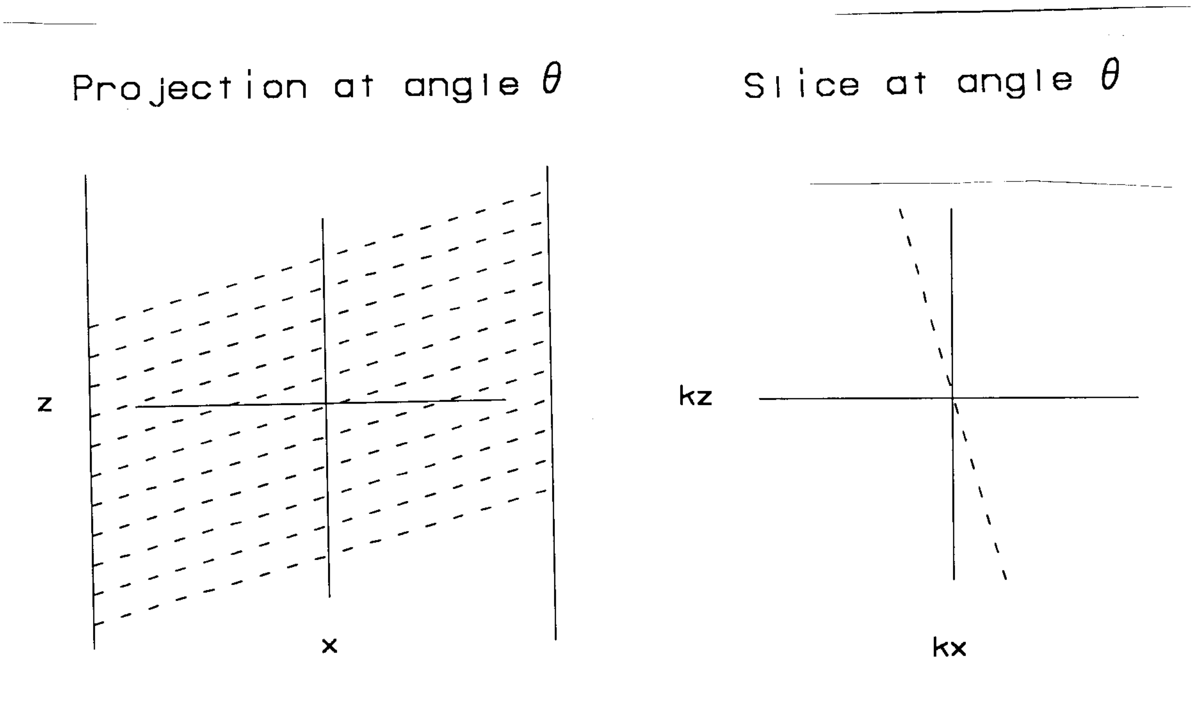

FIG. 3. Projection-slice theorem.

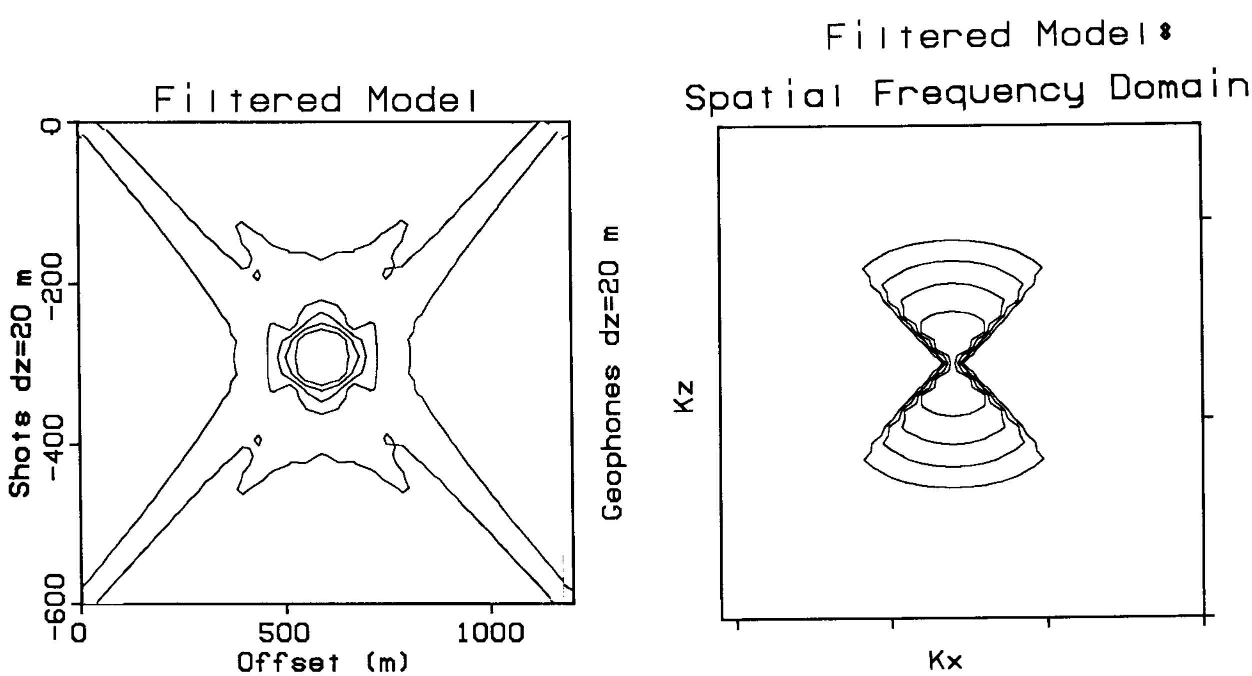

FIG. 4. (a): Pie-slice-filtered amplitude spectrum of Figure 1b. (b): Two-dimensional Fourier transform of (a).

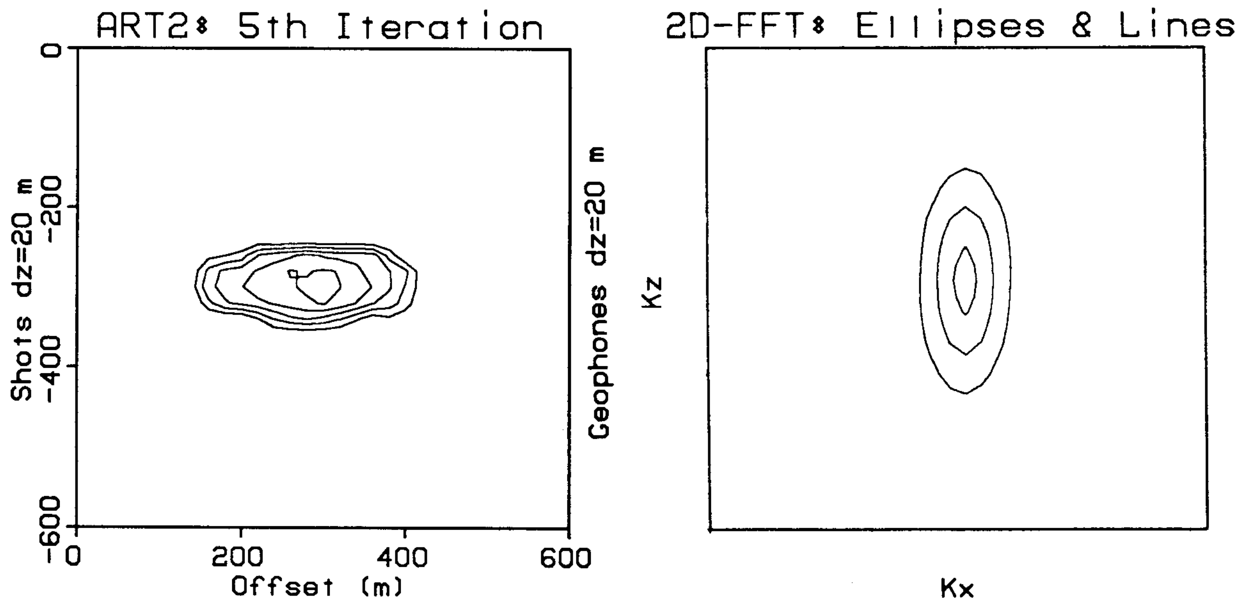

FIG. 5. (a): The fifth iteration in a modified ART solution to the tomography problem posed in Figure 1a. Slowness errors were backprojected along elliptical regions or narrow raypaths—depending on the absence or presence of interference effects in the first pulse after the first arrival. (b): The amplitude spectrum of (a).

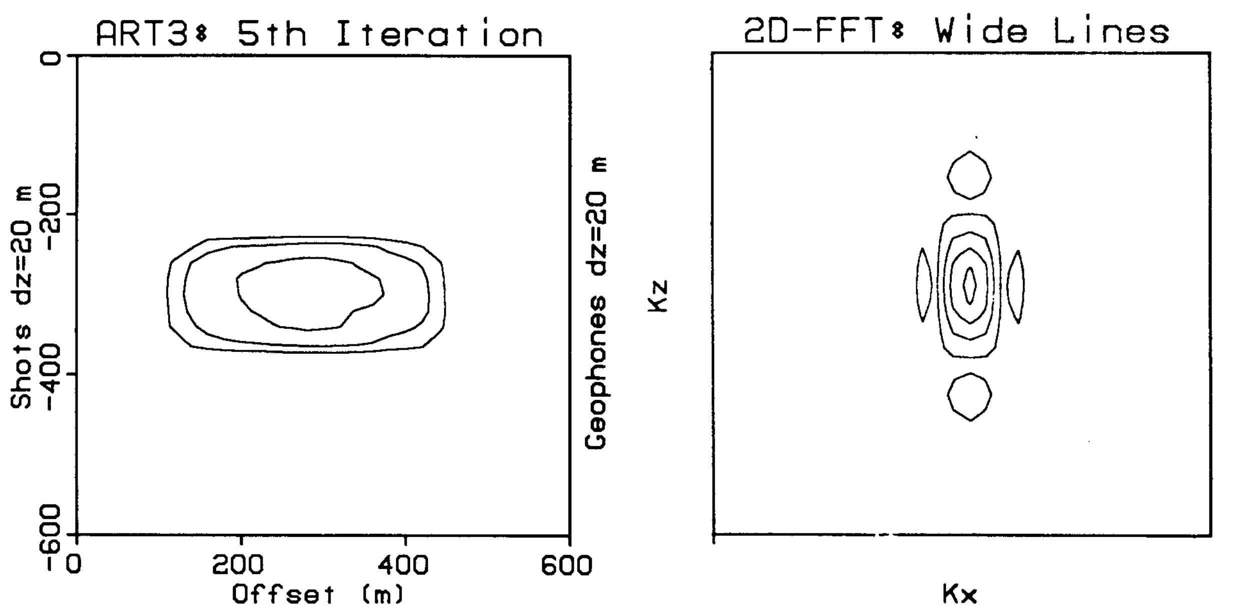

FIG. 6. (a): The fifth iteration in a modified ART solution to the tomography problem posed in Figure 1a. Slowness errors were backprojected along wide raypaths. (b): The amplitude spectrum of (a).

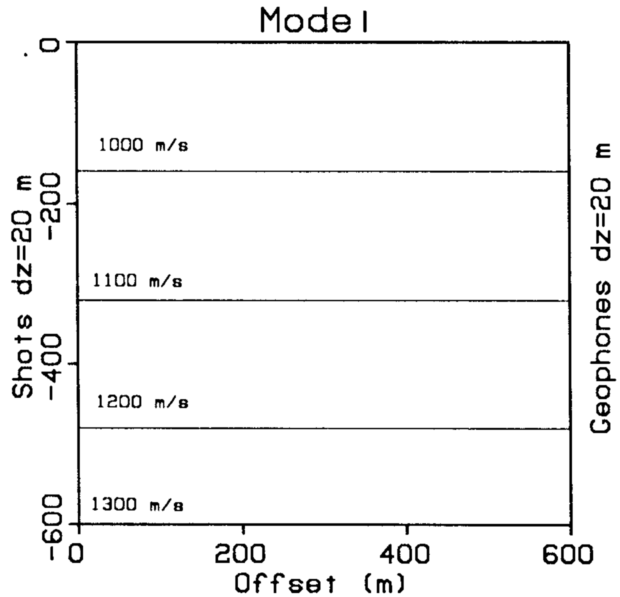

FIG. 7. A flat-layered crosshole tomography experiment.

near vertical projections of the medium slowness, horizontal slices through the two-dimensional transform of the medium slowness function lie in the null space. This point is further illustrated in Figure 4, which shows both the amplitude spectrum of the original model after application of a pie-slice filter similar to that apparent in the ART solution, and its inverse Fourier transform. Pie-slice filtering clearly produces the x-shaped artifacts in the space domain. The effect is more pronounced here than in Figure 2b because the filter was more sharply truncated; raybending in the real experiment smoothed the filter's edges.

The second inversion scheme described in the previous paper is represented by Figure 5a, repeated from Figure 5 in SEP-48. It shows the fifth iteration in a modified ART solution of the problem, where slowness errors were backprojected along either elliptical regions or narrow raypaths—depending on the absence or presence of interference effects in the first pulse after the first arrival. X-shaped artifacts are absent from this figure because the method constrained the solution with information distinct from first break traveltimes, filling the null space with additional information and increasing the linkage between cells. This relation is apparent in Figure 5b, which illustrates the amplitude spectrum corresponding to Figure 5a. While high frequencies in the x-direction remain lost, the notch along the $k_z = 0$ axis has been filled in.

Figure 6a is repeated from Figure 7 in SEP-48, corresponding to the third inversion scheme described in that paper. It again shows the fifth iteration in an ART inversion of Figure 1a's experiment, modified this time to backproject slowness errors along wide raypaths. Figure 6b shows the amplitude spectrum corresponding to this solution. By smoothing in a direction perpendicular to the raypaths, the method low-pass filtered sharp truncations in the frequency domain;

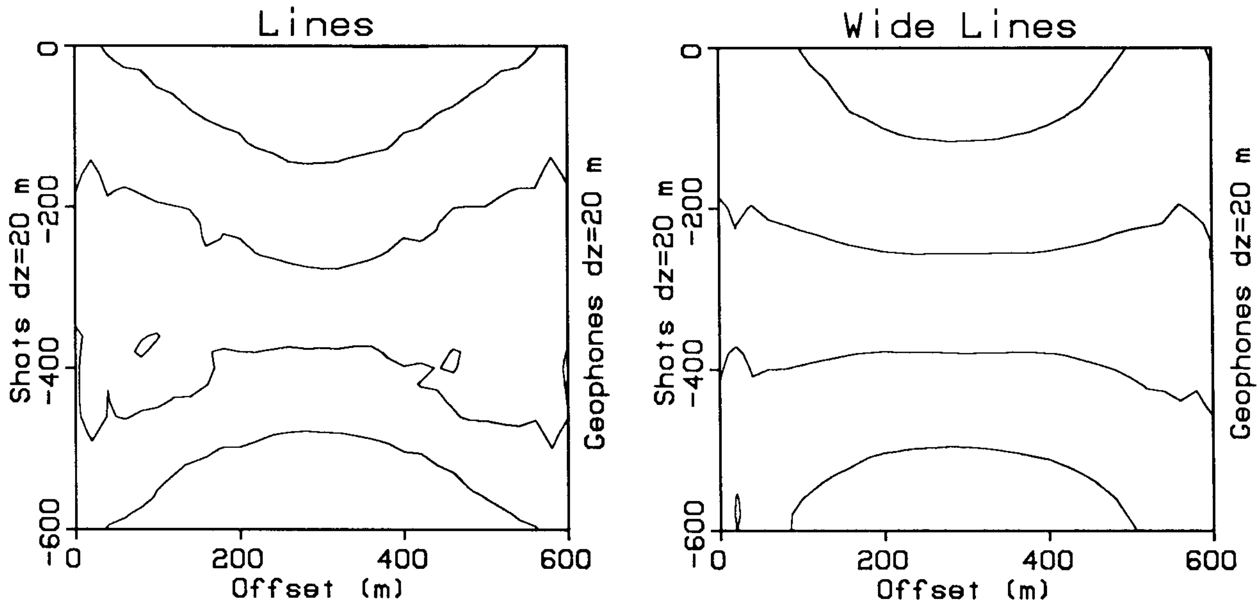

FIG. 8. (a): The fifth iteration in an ART solution (backprojection along narrow raypaths) to the problem posed in Figure 7. (b). The fifth iteration in a modified ART solution (backprojection along wide raypaths) to the same problem.

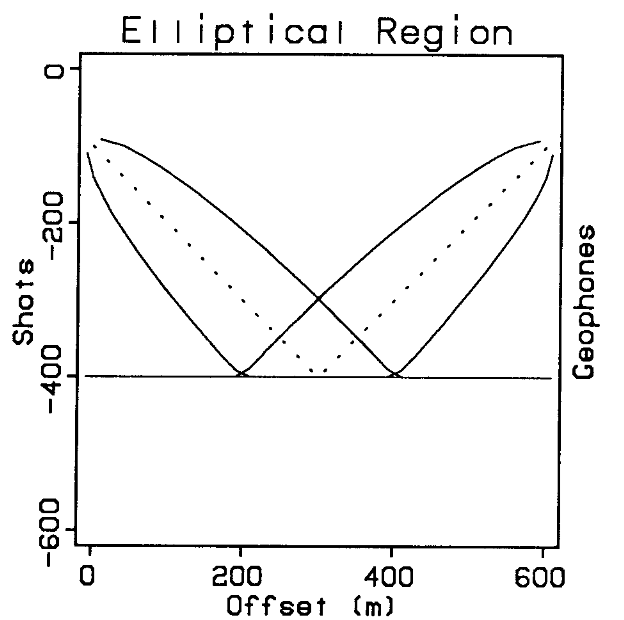

FIG. 9. The elliptical region affecting the first pulse of a reflected wave, adapted from Hagedoorn (1954).

the notch of Figure 2b has been filled in at the expense of high frequencies in both the x and z directions—with a loss of resolution in the space domain.

LAYERED MODEL

In SEP-48 the three modified ART schemes were applied to a single experimental model—the central velocity anomaly case of Figure 1a. The basic ART scheme and the scheme modified to backproject slowness corrections along wide raypaths were also subsequently applied to the flat-layered model of Figure 7. Figures 8a and 8b show the fifth iterations in those inversion schemes, where errors were backprojected along narrow and wide (120 m) raypaths, respectively. Clearly, backprojection along wide raypaths yields a flatter and less artifact-laden solution.

FIGURE CORRECTION

Figure 6a in SEP-48 is in error. It has been corrected in Figure 6.

REFERENCES

Bracewell, R. N., 1956, Strip integration in radio astronomy, Aust. J. Phys., v. 9, p. 198-217.

Woodward, M. J., 1986, Iterative tomography: error projection along ellipses and lines, SEP-48.

190: :	191: :	192: :	193: :	194: :	195: :	196: :	197: :	198: :	199: :
180: :	181: :	182: :	183: :	184: :	185: :	186: :	187: :	188: :	189: :
170: :	171: :	172: :	173: :	174: :	175: :	176: :	177: :	178: :	179: :
160: :	161: :	162: :	163: :	164: :	165: :	166: :	167: :	168: :	169: :
150: :	151: :	152: :	153: :	154: :	155: :	156: :	157: :	158: :	159: :
140: :	141: :	142: :	143: :	144: :	145: :	146: :	147: :	148: :	149: :
130: : ↑	131: : _	132: : ‘	133: : {	134: : │	135: : }	136: : ~	137: : °	138: :	139: :
120:x: Х	121:y: Й	122:z: З	123:{: Ж	124:¦: И	125:}: Ч	126:~: Щ	127: : [	128: : \	129: :]
110:n: Н	111:o: О	112:p: П	113:q: Ю	114:r: р	115:s: С	116:t: Т	117:u: У	118:v: В	119:w: Ш
100:d: Д	101:e: е	102:f: ф	103:g: Г	104:h: Ц	105:i: Ы	106:j: Я	107:k: К	108:l: Л	109:m: М
90:Z: З	91:[: Ж	92:\: И	93:]: Ч	94:^: Щ	95:_: Ъ	96:`: Ь	97:a: а	98:b: б	99:c: э
80:P: П	81:Q: Ю	82:R: Р	83:S: С	84:T: Т	85:U: У	86:V: В	87:W: Ш	88:X: Х	89:Y: Й
70:F: Ф	71:G: Г	72:H: Ц	73:I: Ы	74:J: Я	75:K: К	76:L: Л	77:M: М	78:N: Н	79:O: О
60:<: <	61:=: =	62:>: >	63:?: ?	64:@: ь	65:A: А	66:B: Б	67:C: Э	68:D: Д	69:E: Е
50:2: 2	51:3: 3	52:4: 4	53:5: 5	54:6: 6	55:7: 7	56:8: 8	57:9: 9	58::: :	59:;: ;
40:(: (	41:):)	42:*: Ъ	43:+: +	44:,: ,	45:-: —	46:.: .	47:/: /	48:0: 0	49:1: 1
30: :	31: :	32: :	33:!: !	34:": ″	35:#: #	36:$: $	37:%: %	38:&: &	39:': ’

Font 11

joe, Thu Oct 9 16:34